

Bond Theory

Highs and Lows of Bond Lengths: Is There Any Limit?

Alvaro Lobato,* Miguel A. Salvadó, J. Manuel Recio, Mercedes Taravillo, and Valentín G. Baonza

In memory of Professor Víctor Luaña, Professor Emilio Morán and Professor José Antonio Campo

Abstract: Two distinct points on the potential energy curve (PEC) of a pairwise interaction, the zero-energy crossing point and the point where the stretching force constant vanishes, allow us to anticipate the range of possible distances between two atoms in diatomic, molecular moieties and crystalline systems. We show that these bond-stability boundaries are unambiguously defined and correlate with topological descriptors of electron-density-based scalar fields, and can be calculated using generic PECs. Chemical databases and quantum-mechanical calculations are used to analyze a full set of diatomic bonds of atoms from the *s-p* main block. Emphasis is placed on the effect of substituents in C–C covalent bonds, concluding that distances shorter than 1.14 Å or longer than 2.0 Å are unlikely to be achieved, in agreement with ultra-high-pressure data and transition-state distances, respectively. Presumed exceptions are used to place our model in the correct framework and to formulate a conjecture for chained interactions, which offers an explanation for the multimodal histogram of O–H distances reported for hundreds of chemical systems.

Introduction

Bond distances are recognized as one of the main parameters to describe chemical interactions. Their relationship with bond dissociation energies, bond orders or bond strengths reflects the well-known correlation between atomic-level configurations and macroscopic observable proper-

How to cite: *Angew. Chem. Int. Ed.* **2021**, *60*, 17028–17036
International Edition: doi.org/10.1002/anie.202102967
German Edition: doi.org/10.1002/ange.202102967

ties.^[1,2] Surprisingly, while equilibrium distances have been comprehensively studied, characterized, and tabulated, bond-breaking (or -formation) distances have been marginally explored, even though finding a meaningful relationship between bond properties and bond-breaking distances could provide valuable insights for designing new synthetic routes or improving certain catalytic processes. But characterization of bond-breaking distance and its relationship with equilibrium parameters is a challenging task, since instabilities generally occur in short periods of time, making their experimental detection extremely difficult.^[3–5] In addition, from the point of view of theoretical chemistry, bond breaking (or formation) points require an accurate description of multireference states^[6,7] which sometimes are not easily accessible. Although approaches based on the topological analysis of the electron density^[8] and tailored mechanochemical experiments^[9] have avoided these limitations and have quantified the rupture distances of several bonds in particular molecules, the question “At which interatomic distance a chemical bond disappears?” is still controversial,^[10,11] despite of being crucial to understand and define the extent of chemical interactions and reactivity.^[12–14]

Thus, the definition of the limits of stability of a bond requires finding a general criterion that relates an energetically unstable state with some genuine structural parameter at the molecular level. In this regard, all the energetic states characterizing a certain chemical bond are intrinsically linked to its potential energy curve (PEC), which should reflect the stability constrains. The open question is whether the critical distances associated with the occurrence of an energetically unstable state can be unambiguously defined and accurately determined on the basis of the physical and chemical information contained in the PEC.

Here, we arrive at a practical route to calculate these bond critical distances. The rationale behind our model is the existence of a formally generic analytical function -sometimes referred to as universal^[15–17] -for describing the PEC of a pairwise interaction reference molecule (either in its neutral or charged state). The remarkable simplicity of our model stems from the fact that only energetic and mechanical parameters (dissociation energy and force constant) of a certain chemical bond at its equilibrium configuration need to be known, as we demonstrate through a critical examination of more than 80 diatomic and polyatomic molecules. Examples are worked out to demonstrate convincingly i) the range of distances in which stable single C–C and O–O bonds can exist -irrespective of the charges and substituents involved or the external stimuli applied- and ii) the multimodal distribution found in the O–H distance histogram

[*] Dr. A. Lobato, Prof. M. Taravillo, Prof. V. G. Baonza
MALTA-Consolider Team and Departamento de Química Física,
Universidad Complutense de Madrid
Av. Complutense s/n, 28040 Madrid (Spain)
E-mail: a.lobato@ucm.es

Prof. M. A. Salvadó, Prof. J. M. Recio
MALTA-Consolider Team and Departamento de Química Física
y Analítica, Universidad de Oviedo
Av. Julián Clavería, 8, 33006 Oviedo (Spain)

Prof. V. G. Baonza
Instituto de Geociencias IGEO, CSIC-UCM
28040 Madrid (Spain)

Supporting information and the ORCID identification number(s) for the author(s) of this article can be found under:
<https://doi.org/10.1002/anie.202102967>.

© 2021 The Authors. Angewandte Chemie International Edition published by Wiley-VCH GmbH. This is an open access article under the terms of the Creative Commons Attribution Non-Commercial NoDerivs License, which permits use and distribution in any medium, provided the original work is properly cited, the use is non-commercial and no modifications or adaptations are made.

reflecting changes in the nature of the covalent O–H bond caused by the occurrence of hydrogen bonding or van der Waals interactions with the surrounding atoms.

Results and Discussion

Let us consider a diatomic molecule, the paradigmatic example of a bond PEC. In this case, the bond energy depends only on the interatomic distance. At equilibrium, the bond has a potential energy minimum and is in a stable configuration defined by its equilibrium distance (r_e) and its dissociation energy (D_e). When the bond is compressed, the energy steeply increases up to the zero-energy crossing point, where it changes from negative to positive (see Figure 1). In as much as stable interactions must have a negative potential energy, this point can be considered as the compression stability limit of the bond. In analogy with well-known hard sphere thermodynamic potentials, we will name from now on this zero-energy crossing distance, the hard sphere distance (r_{hs}). It can be interpreted as the closest interatomic distance at which the two atoms of a bond can approach. On the other side, when the bond distance is increased, the potential energy goes to zero asymptotically up to the infinite internuclear distance, where it reaches this value. This point is usually considered as the breaking condition of the bond because no interaction between the atoms exists. Nonetheless, this is not an unstable point in the PEC, but a stable configuration between two non-interacting atoms. Indeed, bond ruptures occur at finite interatomic distances. Hereof, the stretching bond instability must occur somewhere in between the equilibrium point and the point of infinitely separated atoms. Its determination requires a separate discussion.

To be more general, suppose that two bonded atoms of a larger chemical system experience a tensile force along its internuclear distance by means, for instance, of an AFM tip,

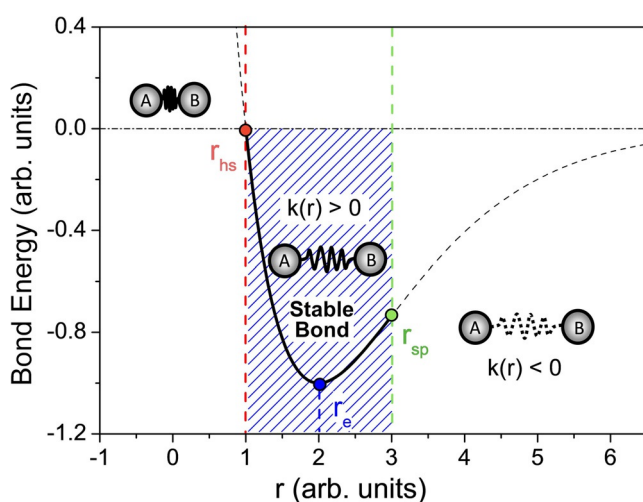


Figure 1. Potential energy curve of a generic A–B diatomic bond. Hard sphere (r_{hs}) and spinodal (r_{sp}) points are represented by red and green dots, respectively, whereas the equilibrium distance (r_e) is represented with a blue point. The stability region of the bond is displayed with the blue shaded area.

electronegative substituents or an attractive chemical interaction. We assume that these stimuli exert a negligible effect on the chemical nature of the diatomic bond, as we move from the equilibrium position in the potential energy curve up to a distance $r > r_e$, always fulfilling the condition of a positive definite energy-hessian. In our pairwise model, the latter condition implies that the second derivative of the energy with respect to the distance, the stretching force constant $k(r)$, must be positive (see Figure 1). $k(r)$ decreases with r up to the inflexion/turning point of the PEC, where its value becomes zero. This distance represents the limit where the attractive interactions cannot balance the external tensile effects and, consequently, the breaking process of the bond begins. The condition of zero stretching force constant must be understood as the mechanical stability limit between the stable and unstable stretching regimes. In resemblance with the thermodynamic realm, where the mechanical stability limit defined by the condition of infinity compressibility is known as the spinodal locus,^[18] we will refer to this diatomic rupture energy and distance as the spinodal energy, E_{sp} , and the spinodal distance, r_{sp} , respectively.

It is worth to mention that the notion of bond rupture through the condition of zero second derivative has been highlighted in the literature in different contexts such as in reaction force analysis,^[19–21] in the study of compliance and adiabatic force constants^[11,22] or in the determination of the maximum force produced in mechanochemical studies.^[23,24]

The performance of the above defined hard sphere and spinodal limits in seventy diatomic molecules was analyzed using their potential energy curves determined from spectroscopic parameters according to the Rydberg-Klein-Rees (RKR) procedure.^[25–29] These data include single, multiple, polar covalent and ionic bonds, as well as different ground state multiplicities. All the computed data along with the parameters used in the RKR potentials are collected in the Supporting Information (SI; see Table S1). In spite of the broad range of critical parameters displayed by our set of molecules in the variety of bond types included in our study, it is striking to see that the calculated E_{sp} , r_{sp} , and r_{hs} limits show quite uniform values when normalized with the corresponding equilibrium parameters. Energy and distance values and uncertainties are, respectively, $E_{sp} = (-0.73 \pm 0.03) D_e$, $r_{sp} = (1.27 \pm 0.07) r_e$, and $r_{hs} = (0.73 \pm 0.07) r_e$. Similar results are obtained when a separated examination of diatomics involving noble gas atoms is carried out (see Figure S1 in the SI).

The fact that our normalized boundary parameters (E_{sp}/D_e , r_{sp}/r_e , and r_{hs}/r_e) present low fluctuations has not to be associated with any merit of our analysis, but with a natural consequence of the general shape of pairwise interaction curves. Indeed, the claim of a pairwise universal binding energy relationship (UBER) was previously disclosed in the seminal papers of Rose and co-workers,^[15–17] where they demonstrate that a Rydberg type PEC describes pairwise binding properties in molecules, covalent and ionic crystals, metals, and chemisorbed species. Specifically, the proposed UBER reads:

$$E/D_e = -(1 + a^*)e^{-a^*} \quad (1)$$

where a^* is a scaled distance defined in terms of the dissociation energy, D_e , and the equilibrium stretching force constant k_e :

$$a^* = \frac{r - r_e}{(D_e/k_e)^{1/2}} \quad (2)$$

In this analytical potential, the hard sphere and spinodal conditions are evaluated through the particularly simple conditions $a^* = -1$ and $a^* = +1$, respectively, and are easily derived just requiring the energy and the second derivative of the energy with respect to the distance, to be zero. Accordingly, E_{sp} and the difference and the sum between r_{hs} and r_{sp} can be expressed as:

$$E_{sp} = -D_e 2e^{-1} = -0.736D_e \quad (3a)$$

$$r_{sp} - r_{hs} = 2 \left(\frac{D_e}{k_e} \right)^{1/2} \quad (3b)$$

$$r_{sp} + r_{hs} = 2r_e \quad (3c)$$

Not fortuitously, the UBER potential predicts a multiplicative factor of -0.736 for the ratio between E_{sp} and D_e , within our average -0.73 ± 0.03 value range obtained from the spectroscopic data. It is not the first time that the constancy of the E_{sp}/D_e ratio is highlighted as a noteworthy feature of the PEC. Using the term activation energy of the bond instead of our spinodal energy, Politzer and Murray et al. arrived at a similar result in their study of the reaction force along the diatomic bond rupture.^[30,31]

A word of caution is needed here to avoid misunderstandings concerning the validity of the above relationships. First, the interatomic potential is accurately described not only in terms of the UBER curve but also with other standard analytical equations as, for example, the Morse or the Lennard-Jones potentials (see SI). And second, this description assumes that the dissociation path does not involve crossing states nor is meaningfully affected by electron reorganization effects. In the set of neutral *sp*-type diatomic molecules selected in our analysis, the dissociation energy corresponds closely to the intrinsic dissociation energy defined by Cremer et al.^[32] This means that most of our molecules keep the nature of the interaction along the dissociation path as they have at equilibrium and, thus, the fulfilment of Equation (3) is expected. However, in those cases where the dissociation state leads to an apparent or effective dissociation energy, which necessarily differs from the intrinsic dissociation energy, as in some transition metal diatomic molecules or in highly charged species (like the O_2^{2+} cation that we discuss later), the evaluation of bond length limits could not be so straightforward.

Regarding r_{sp} and r_{hs} distances, our UBER analysis leads to an expression [Eq. (3b)] that only depends on equilibrium parameters of the bond (k_e , D_e , and implicitly r_e). This is graphically verified in the plot of Figure 2. An illustrative linear correlation between our calculated bond limits and the empirical $(D_e/k_e)^{1/2}$ values is obtained with a slope of (2.06 ± 0.03) , very close to the formal value of 2 in Equation (3b). Under this view, bond ruptures reveal to occur at particular

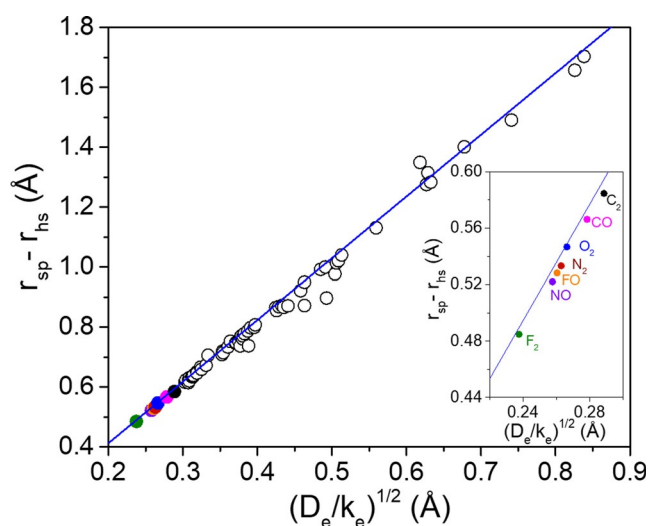


Figure 2. Difference between spinodal (r_{sp}) and the hard-sphere distances (r_{hs}) against the $(D_e/k_e)^{1/2}$ scaling parameter of the UBER potential for several diatomic molecules: Al_2 , $AlCl$, AlF , AlH , AlO , AlS , B_2 , BCl , $BeCl$, BeF , BeH , BeO , BeS , BF , BH , BN , BO , BS , C_2 , CCl , CF , CH , Cl_2 , ClF , ClH , $ClLi$, ClO , $ClSi$, CN , CO , CP , CS , F_2 , FH , FLi , FMg , FN , FNa , FO , P_2 , FS , FSi , H_2 , HLi , HMg , HN , HNa , HO , HP , HS , $LiNa$, Mg_2 , MgO , MgS , Na_2 , N_2 , NO , NP , NS , NSi , O_2 , OP , OS , Osi , P_2 , Si_2 , S_2 , and SSi . The straight line corresponds to the equation $(r_{sp} - r_{hs}) = (2.06 \pm 0.03) (D_e/k_e)^{1/2}$. Colored symbols highlight diatomic molecules with rupture distances closer to their equilibrium values and are displayed in the inset.

distances that depend on bond equilibrium features. Indeed, k_e , and D_e have been usually considered chemical descriptors of the bond strength.^[33] Both parameters are widely used across the literature to explain bond length-bond strength correlations,^[34] although which one has to be used is also a matter of debate.^[2] However, as emphasized by Kaupp et al.,^[2] an operative definition of bond strength would recall in its capacity to predict how easy a chemical process progresses as a result of a change in bond lengths. In this regard, our results evidence that bond ruptures depend on the combination of both parameters. The dissociation energy measures the cost to separate the atoms, whereas the equilibrium force constant, the curvature of the PEC, represents the rate in the increasing energy as the bond is distorted.

Accordingly, those rigid bonds with high stretching force constants that have low dissociation energies should display rupture distances close to their equilibrium values. From this point of view, a connection between the Hammond postulate^[35] and the spinodal stability limit is provided since the particular bonds identified in this postulate are detected in our model. We realize that in our set of diatomic molecules the smaller differences between the spinodal and the hard sphere distances, or equivalently the smaller $(D_e/k_e)^{1/2}$ ratios, are found in those molecules with multiple and halogen bonds such as F_2 , NO , FO , N_2 , O_2 , CN , and C_2 (highlighted in Figure 2). In as much as these results are independent of the diatomic potential used (other potential energy functions can be easily checked to provide an equivalent plot), we can use

the bond stability limits as a reference to define bond ruptures along chemical processes.

Our next step concerns whether a relationship between the energetic-mechanical instability and the electronic structure associated with a bond rupture can be provided. To do that, we examine the topology of two popular scalar fields, the electron density (ρ)^[36,37] and the electron localization function (ELF),^[38,39] frequently used to characterize bond breaking processes, chemical reactions,^[8,40,41] and phase transitions in solid state.^[42,43]

During the rupture of a covalent bond, shared electrons migrate from the internuclear axis to the respective atoms giving as a result two interacting but not bonded radicals.^[8] In the same way, when the molecule is compressed up to the limit where the electronic repulsion dominates, the bonding electrons suffer a strong confinement in a really tiny space, the cores began to repel with each other and, formally, the bond disappear forming an inner valence shells interaction. The activation of the core electrons at the hard sphere point would have a deep impact in the ionization potential or in the electronegativity of the atoms, as previously noticed in the high-pressure field.^[44–47]

It is known that the electron density along the internuclear region of homonuclear diatomics usually experiences a transition from a first-order saddle point (bonding point) to a non-nuclear maxima (NNM) under compression.^[48] In our calculations in several homonuclear bonds, this signature change of ρ at the bond critical point precisely appears at distances never higher than ± 0.15 Å of our predicted r_{hs} values (see Table S2 and Figure S2).

The confirmation of this mechanical-electronic correlation cannot be extended to heteronuclear diatomic bonds since, as discussed by Pendás et al.^[48] and others,^[49] the occurrence of NNMs in these cases is less likely. However, the expected core effects at the r_{hs} limit should be produced in a similar way as in homonuclear bonds. Thanks to the ELF, a quantitative account of this situation can be also disclosed. Taking as an example the C–O bond in ethanol, we illustrate in Figure 3 how the ELF C–O bond attractor suffers a cusp catastrophe in the compressed state transforming into a saddle point and two new attractors. Furthermore, each of these new ELF basins yields $0.8e^-$. These topological changes in the index of the ELF bond attractor and concomitant increasing of the e^- populations when the C–O bond is squeezed from its 1.45 Å equilibrium distance to 0.8 Å along the bond axis, are

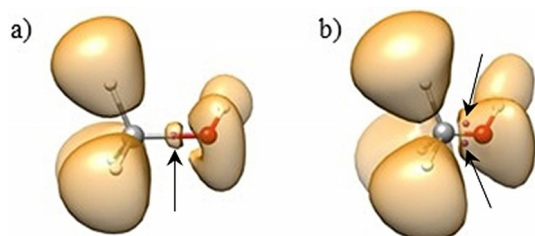
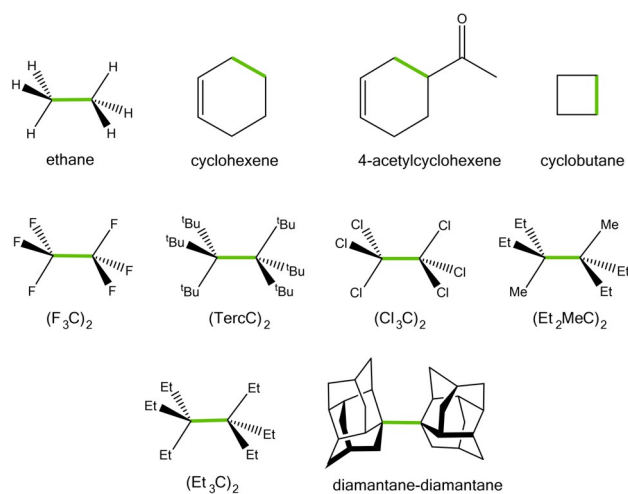


Figure 3. ELF isosurfaces in beige for CH₃OH (ELF isovalue 0.78) along with bond attractors represented as small purple spheres identified by arrows at C–O distances of a) 1.45 Å and b) 0.95 Å. White, grey, and red balls stand for H, C, and O, respectively.

also representative of what happens in the heteronuclear bonds of our study. In spite of the reduced number of selected bonds and that no more exhaustive analysis were carried out with alternative descriptors (HOMO–LUMO gaps,^[50] natural bond orbital electron populations,^[51] the effective number of unpaired electrons,^[52] etc.), we dare to conclude that the emergence of both, NNMs and the ELF topological singularities, are electronic evidence of the mechanical-energetic hard sphere limit.

The connection between bond stability limits and special electron density topological features becomes more difficult to carry out in the analysis of the rupture distances. We are aware that static correlation effects are important when the shared electrons of a bond have to be distributed into the two dissociation fragments. The monodeterminantal description is not enough and an electronic complete active space (CAS) involving orbitals of the two fragments should be at least incorporated in the calculations.^[53–55] Such calculations are out of the scope of this work, requiring a separate analysis elsewhere. Nevertheless, the use of ELF topological signatures points toward a (likely fortuitous) correlation between mechanical and electronic descriptors at the distance where the rupture is predicted in sigma covalent bonds. Results in molecules computed at a CCSD level are shown in Table S2 and Figures S2 and S3 in the SI. The difference between the distance r_{BET} where the ELF bond disynaptic basin disappears (a cusp or fold catastrophe according to the bonding evolutionary theory, BET),^[8,56,57] and r_{sp} is usually smaller than 0.05 Å. Overall, we find that the spinodal distances are in very good agreement with the BET cusp catastrophe ones. According to these results, covalent interactions could not be extended far beyond their unique bond spinodal distances because they are both mechanically and electronically unstable.

We now seek the application of our scheme to the determination of the limit distances at which σ C–C covalent bonds in stable compounds can be found. On this basis, we have calculated using the B3LYP-DFT approach (see details and Figure S4 in the SI) the pure stretching potential energy



Scheme 1. Molecules and C–C bonds (marked in green) studied in this work.

Table 1: Mechanical (r_{hs} , r_{sp}) and electronic rupture (r_{NNM} , r_{BET}) distances for the C–C bonds of the molecules summarized in Scheme 1. All units are in Å. r_{NNM} stands for non-nuclear maxima distance and r_{BET} stands for the distance where the ELF-BET catastrophe occurs.

C–C Bond	r_{hs}	r_{NNM}	r_{sp}	r_{BET}
Ethane	1.08	1.10	1.99	2.00
Cyclohexene	1.15	1.10	1.96	1.95
4-Acetylcyclohexene	1.09	1.10	1.98	2.00
(F ₃ C) ₂	1.13	1.20	1.99	2.00
Cyclobutane	1.11	1.10	1.99	1.95
(TercC) ₂	1.16	1.10	2.03	2.05
(Cl ₃ C) ₂	1.13	1.15	2.03	2.10
(Et ₂ MeC) ₂	1.17	1.15	2.05	2.05
(Et ₃ C) ₂	1.15	1.15	2.08	2.10
Diamantane–diamantane	1.22	1.20	2.13	2.15

curves for selected C–C bonds in a series of organic molecules (see Scheme 1) and we have determined the distances at which mechanical and electronic instability occur (see Table 1). While it is true that the equilibrium bond electronic properties are modified by the substituents, our electron density and ELF analysis reveal that the σ C–C bond rupture mechanism proceed in a similar fashion. Despite of the presence of huge inductive and negative hyperconjugation effects, highly strained bonds or dispersive interactions, the limiting distances, r_{hs} and r_{sp} , show small deviations with average values of 1.14 ± 0.04 Å and 2.02 ± 0.05 Å, respectively. If we focus on the C–C σ covalent bond of the reference ethane molecule similar values are obtained. Notice also that the average NNM and BET distance (1.13 ± 0.04 Å and 2.03 ± 0.06 Å, respectively) make all the data to be consistent with each other.

As regards the upper limit, several sources point to a value never higher than 2.2 Å. See for example the C–C distance histogram of Isea^[58] collecting all the C–C bonds contained in the Cambridge Structural Database.^[59] It is also remarkable that, in the study of the diamino-o-carborane compounds which contain the longest C–C bond synthesized to date,^[60] the authors claimed the existence of a bond path between the longest C–C bonds that disappeared also at 2 Å. Likewise molecular dynamics, time resolved ultrafast spectroscopy, and electron density studies have shown that in Diels–Alder reactions both symmetrical and unsymmetrical transition states involve constant C–C bond distances distributions between 1.9 to 2.2 Å.^[4,61,62] These different criteria indicate that σ C–C covalent interactions are broken or formed at a similar distance (≈ 2 Å) and constitute an empirical proof of the plausibility of our predicted C–C high-rupture spinodal limit.

The lower limit brings into the discussion the possibility of considering C–C bond types other than the σ covalent bond of the reference ethane molecule. We notice that even ultra-short C–C single bonds produced by confinement and van der Waals (repulsive) forces^[63] (≈ 1.3 Å) or in molecules with double (≈ 1.3 Å) and triple (≈ 1.2 Å) bonds, C–C distances are never found lower than our r_{hs} limit (1.14 ± 0.04 Å). This boundary could be used to predict the stability limit of diamond at ultra-high pressure. Up to now, experiments

carried out by Occelli et al.^[64] at 140 GPa have reported that the C–C distance in diamond at this pressure is about 1.43 Å. Likewise, computer simulations find that the lowest C–C distance before the transition of diamond to the *bc8* structure at 1 TPa is 1.23 Å,^[65] again above our r_{hs} limit.

A particular situation that is detailed in the SI (Figure S5) may appear if charge or substituents induce a change in the mechanical properties of the chemical interaction considered. In this case, the bond stability limits and, consequently, the corresponding spinodal and hard sphere distances may be modified when compared to those obtained for σ covalent C–C bonds. We observe that bond stability limits derived from a reference molecule (e.g., ethane for σ (C–C) covalent bonds) are unique for that specific bond type. In contrast, any change in the bonding nature of a given compound (e.g., charge induced in the ethane cation radical discussed in the SI), alters the mechanical properties of the bond and the potential energy function and their bond stability limits are accordingly modified. However, and this is quite relevant, such modified limits do exist and are also unique for those bonds displaying the same type of interaction.

As we have anticipated, the O₂²⁺ cation represents another challenging example, since the energy associated with the dissociation state differs from the intrinsic dissociation energy; here the strong Coulombic repulsion of this chemical species prevents a continuous dissociation path keeping the same electronic organization as in the equilibrium bonding state. Therefore, defining the associated hard sphere state from such dissociation energy reference is meaningless. However, the fact that the bond dissociation energy is ill-defined does not mean that a reference hard sphere point does not exist. It is an intrinsic characteristic of a PEC displaying a minimum, as demonstrated by Wang^[66] and corroborated by our results. In the case of O₂²⁺, the hard sphere point can be estimated using the equilibrium and spinodal distances, which are barely influenced by the dissociation path or the dissociation reference state.

Using the data provided by F. Fantuzzi et al.,^[67] we have numerically computed the energy second derivative as a function of the internuclear distance for O₂²⁺. This curve presents a spinodal point at 1.31 Å evidencing the rupture of the O₂²⁺ bonding interaction at this distance. When this value and the equilibrium distance (1.06 Å) enter Equation (3c), a value around 0.81 Å is estimated for the hard sphere distance, and an intrinsic dissociation energy of about 200 kcal mol^{−1} is obtained. All these results are shown in the Figure S6 in the SI. As it can be seen in this Figure, using the estimated intrinsic bond dissociation energy as a reduction parameter, the O₂²⁺ curve overlaps quite well with those corresponding to prototypical molecules as O₂, F₂O₂ and H₂O₂, at least in the meaningful distance range of O–O stability. This is defined by the calculated hard sphere and spinodal points that occur at similar values in r_e reduced units (0.766 and 1.28, respectively). Since the O₂²⁺ cation displays the shortest bond length among molecules not containing H or He,^[68] it is a good example to verify if it can be accounted for by our model. The stability limits of the neutral O₂ molecule (calculated from the RKR data showed in the SI as a reference) is used to construct the diagram of distances

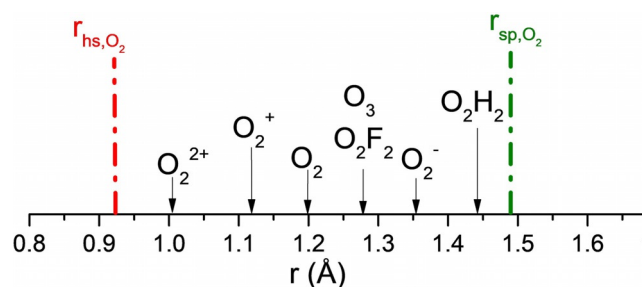


Figure 4. Diagram comparing the hard-sphere (red line) and the spinodal (green line) distances of the O_2 molecule with equilibrium distances found in different $\sigma(O-O)$ bonds (vertical arrows).

depicted in Figure 4. One can see that charged molecules, such as the O_2^{2+} , O_2^+ , O_2^- , and others substituted, like F_2O_2 or O_2H_2 , show the expected trend in bond lengths with values all falling within the limits predicted by our model.

Up to now we have demonstrated that single covalent bonds display chemical meaningful bond limits. However, can these criteria be generalized to define the boundaries of other different types of interactions? It is reasonable to suppose that the nature of interactions between two atoms at a given distance can be revealed by clear features of the electronic density. For instance, Espinosa et al.^[69,70] demonstrated in a series of works that interatomic interactions can be grossly classified according to three different scenarios. The covalent regime appears at short interatomic distances where the valence shells are shared. It is characterized by a negative value of the Laplacian of the electron density. At higher distances, the beginning of the electrostatic regime corresponds with the point where the Laplacian of the electron density displays a positive value at the bonding critical point, evidencing that valence shells are separated. Espinosa et al. found that this signature is maintained at longer distances, but when the electronic kinetic energy density overcomes the value of the potential energy density at the bonding critical point then the regime of weak dispersive or van der Waals interactions between pure closed shells starts.^[69]

H-bonds deserve a separate discussion as they are the focus of continuous debate and controversy (see for example references^[71–73] and references therein). Moreover, we will specifically deal with this interaction in our example below. Grabowski et al.^[71] studied the distance interval of a covalent O–H interaction and determined this range to occur up to distances of 1.25 Å. Distances at which pure O–H covalent interactions extend, were also pointed out by Dominiak^[74] and Espinosa.^[69,70] Interactions with positive values of the Laplacian of the electron density and both negative and positive energy densities have been associated to strong and weak hydrogen bonds, respectively. In those cases, an electrostatic contribution dominates the bonding due to the closed shell nature of the atoms displayed by the electron density distribution but with a substantial covalent degree if the energy density is negative. Typically, strong and weak hydrogen bonds have been classified to occur up to distances of 2.4 Å.

From a chemical point of view, each of the above regimes has its own energetic and mechanical properties, and there-

fore each must be represented by a different PEC. Combining this reasoning within our scheme of “high and lows” in bond lengths, we conjecture about the occurrence of chained-interactions of varying nature and strength. This scenario would open up the possibility of widening our scheme to crystalline systems dominated by covalent, H-bond or van der Waals interactions.

To check this idea, we have analyzed the three scenarios in which O–H interactions^[74,75] (covalent, H-bond and van der Waals) are commonly involved. Accordingly, we assume that when a covalent O–H bond elongates towards its spinodal point, the H-bond interaction ($O\cdots H$) comes into play. If we now consider the ($O\cdots H$) interaction compressed towards its hard sphere limit, the instability must coincide with the covalent spinodal limit, since the covalent and H-bond interactions are concatenated. A similar reasoning can be applied to the transition between the ($O\cdots H$) interaction and the subsequent van der Waals-like interaction. Figure 5 (top panel) renders a schematic picture of our conjecture for chained O–H interactions. In analogy with reactive schemes,

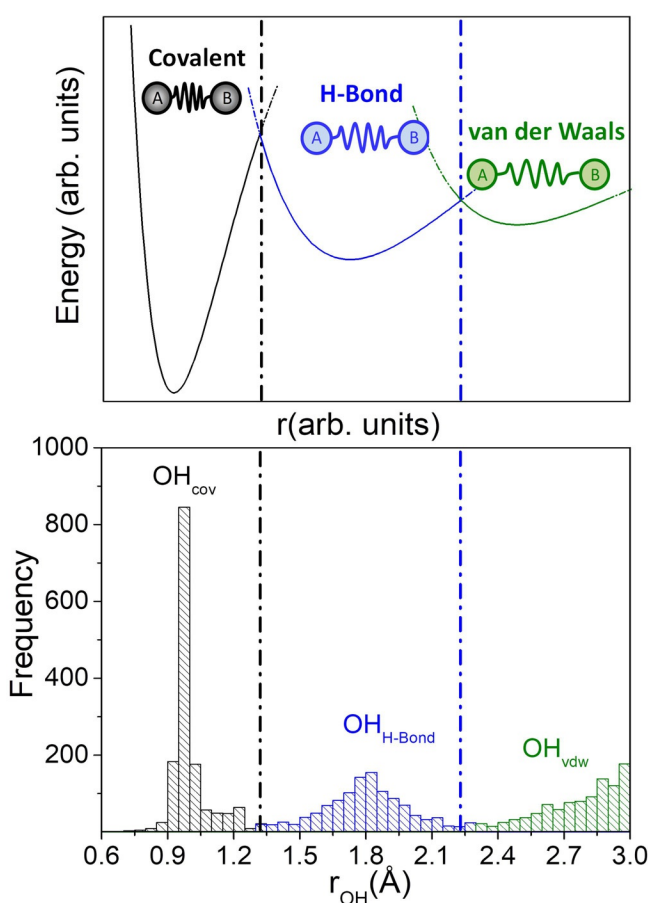


Figure 5. (Top panel) Schematic representation of the chained interaction conjecture. In black, the covalent bonding, blue and green represents the electrostatic and van der Waals interaction regimes, respectively. Notice how the spinodal limit corresponds to the hard-sphere distance of the next interaction. (Bottom panel) Distance histogram for the O–H interaction, bin width = 0.05 Å. Covalent, H-Bond, and van der Waals contacts have been represented as black, blue, and green bins, respectively. Dash-dotted lines correspond to $r_{sp,covalent} = r_{hs,H-bond} = 1.36$ Å and $r_{sp,H-bond} = r_{hs,vdW} = 2.14$ Å.

where the crossing between two PECs defines a transition state, we refer to these distances as bonding transition regions.

The profound implications of our model are evident by analyzing a statistically significant number of O–H interactions over a wide distance sampling interval, as depicted in Figure 5 (bottom panel), where we observe a well-defined pattern of maxima and minima identifying the three different types of O–H interactions. Ultimately, our model of chained interactions provides more than a satisfactory interpretation of the multimodal distribution of the histogram of number of O–H contacts as a function of the distance for all the compounds included in the Cambridge crystallographic database.^[8] For ease of discussion, we have differentiated covalent bonds (black boxes) from non-covalent interactions (blue and green boxes).

Now, solving Equation (2) for $a^* = 1$ (r_{sp}) and $a^* = -1$ (r_{hs}), we obtain explicit expressions for the two critical distances:

$$r_{\text{sp}} = r_{\text{c}} + (D_{\text{e}}/k_{\text{e}})^{1/2} \quad (4a)$$

$$r_{\text{hs}} = r_{\text{c}} - (D_{\text{e}}/k_{\text{e}})^{1/2} \quad (4b)$$

The consistent values of $(D_{\text{e}}/k_{\text{e}})^{1/2}$ discussed earlier for a wide range of compounds allows us to calculate r_{hs} and r_{sp} for the three O–H interactions (covalent, H-bond and van der Waals) assuming a common $(D_{\text{e}}/k_{\text{e}})^{1/2}$ value of 0.39 Å. For instance, in the water molecule, D_{e} and k_{e} are 500 kJ mol⁻¹ and 6.1 N cm⁻¹, respectively ($(D_{\text{e}}/k_{\text{e}})^{1/2} = 0.37$ Å), whereas in the water dimer the corresponding values associated with the hydrogen bond interaction are 20 kJ mol⁻¹ and 0.197 N cm⁻¹ ($(D_{\text{e}}/k_{\text{e}})^{1/2} = 0.42$ Å).

Accordingly, using $r_{\text{c}} = 0.97$ Å, which corresponds to the sum of the O and H covalent radii provided by Pyykkö,^[76] Equation (4) yields $r_{\text{hs, cov}} = 0.58$ Å and $r_{\text{sp, cov}} = 1.36$ Å for the covalent interaction.

As the chained-interaction conjecture implies that $r_{\text{sp, covalent}} = r_{\text{hs, H-bond}}$, a value for the $r_{\text{e, H-bond}}$ and $r_{\text{sp, H-bond}}$ can be straightforwardly obtained by rearranging Equations (4a) and (4b) ($r_{\text{e, H-bond}} = 1.75$ Å, $r_{\text{sp, H-bond}} = 2.14$ Å). Following the same procedure, we obtain $r_{\text{e, vdW}} = 2.53$ Å and $r_{\text{sp, vdW}} = 2.92$ Å.

Since our covalent reference distance was determined from the Pyykkö radii, it coincides with the first maximum in the distribution. More interestingly is the position of the first minimum. It occurs in a range between 1.2 and 1.4 Å. Our predicted covalent spinodal distance of 1.36 Å clearly lies in this interval and is also in good agreement with the values of Grabowsky et al.^[71] and Espinosa et al.^[69] The number of contacts produced at this distance is less than 20 units in more than 1000 compounds. Moreover, this distance is not a statistically favored one neither for covalent nor for electrostatic interactions. To the best of our knowledge the empirical presence of such a minimum in the histogram has not been theoretically justified yet. Here, we realize that such a distance corresponds to the covalent spinodal limit or equivalently to the hard sphere boundary of the H-bond interaction. Our model is revealing that these mechanically unstable geometries are not favored, and therefore few compounds are expected with O–H distances around 1.36 Å.

Concerning the H-bond interaction, we observe that the maximum in the histogram (1.75–1.85 Å) occurs close to our predicted H-bond equilibrium length (1.75 Å). Notice that we have calculated this value only from the O–H covalent equilibrium distance and a constant value for $(D_{\text{e}}/k_{\text{e}})^{1/2}$. As regard the second minimum in the multimodal distribution around (2.1–2.4 Å), we again find that our model predicts a H-bond-van der Waals transition within this range (2.14 Å). Finally, our model predicts another maxima and rupture distance for a van der Waals interaction. The latter it is not observed in the distance diagram mainly because, as it has been pointed out by several authors,^[77,78] it includes a monotonically increasing non-contact distance distribution which modify the statistics of this regime. However, it is worth to highlight that our chained interaction model predicts a van der Waals spinodal distance of 2.92 Å, only 0.08 Å lower than the sum of the O and H van der Waals radii predicted by Alvarez et al.^[77] and 0.33 Å larger than the estimations provided by electron density analysis.^[79]

These results provide a first demonstration that the bonding characteristics of two atoms evolve with the distance in a chained fashion, as imposed by the stability conditions of the corresponding interaction. From this point of view, covalent bonds, hydrogen bonding and dispersive interactions behave formally in the same way with respect to the occurrence of critical distances (hard sphere, equilibrium and spinodal).

Conclusion

The analysis of the inherent mechanical and energetic characteristics of a generic PEC allowed us to discuss the minimum (hard sphere) and maximum (spinodal) distances at which a given chemical bond can be considered stable. A first attempt to validate this new framework has been provided by a combined analysis of spectroscopic data and electronic structure calculations in more than 80 diatomic and molecular species. Changes in topological descriptors of scalar fields related to the electron density around bond stability boundaries have been observed, although more accurate and rigorous calculations are still needed to demonstrate this fully conclusively. For practical purposes, we have devised a simple method for calculating the limiting bond distances, which only resorts to the bond strength parameters (k_{e} and D_{e}). Our model does not depend on the particular PEC function (UBER, Morse, Lennard-Jones, etc.) since it only assumes a bonding shape of the pairwise interaction.

When applied to C–C and O–O covalent bonds, we found that bond lengths reported so far in different experiments and computational simulations lie within the boundaries predicted by our model. We also address the difficulties related to bonds with ill-defined dissociation energies, which, however, can be accounted for in our model considering intrinsic bond dissociation energies as we discussed in the O₂²⁺ dication.

Within this framework, we introduce a chained-interactions conjecture that we checked in the ubiquitous O–H pair interaction. We suggest that bond ruptures are concatenated, thus defining a covalent/H-bond/van der Waals sequence that

successfully explains the maxima and minima found in the O–H histogram of distances observed experimentally. Histograms of interatomic distances have been used to generate covalent radii,^[80] but it is the first time that they are interpreted in terms of stability limits.

These results could be used as a guide to determine the distances that will be unreachable (unstable) in the laboratory and anticipate restrictions to the synthesis of novel compounds (either molecules or crystals).

Acknowledgements

This work was supported by the Spanish National Research Agency (AEI) through projects PGC2018-094814-B-C21, PGC2018-094814-B-C22 and RED2018-102612-T, and Principado de Asturias FICYT under Project No. FC-GRUPIN-IDI/2018/000177. We acknowledge Prof. Ángel Martín-Pendás for fruitful discussions, Dr. David Abbasi (Silico Studio) for designing the TOC Figure and Billy Shears for inspiration. We also thank the anonymous referees for pointing out working examples and suggestions for improving the content and broadening the scope of our study.

Conflict of interest

The authors declare no conflict of interest.

Keywords: bond length · carbon–carbon bonds · ELF (electron localization function) · hydrogen bonds · potential energy curve

- [1] L. Pauling, *The nature of the chemical bond and the structure of molecules and crystals: An introduction to modern structural chemistry*, University Press, Ithaca, **1960**.
- [2] M. Kaupp, D. Danovich, S. Shaik, *Coord. Chem. Rev.* **2017**, *344*, 355–362.
- [3] T. Bredtmann, M. Ivanov, G. Dixit, *Nat. Commun.* **2014**, *5*, 5589.
- [4] K. Black, P. Liu, L. Xu, C. Doubleday, K. N. Houk, *Proc. Natl. Acad. Sci. USA* **2012**, *109*, 12860–12865.
- [5] W. Li, A. A. Jaraón-Becker, C. W. Hogle, V. Sharma, X. Zhou, A. Becker, H. C. Kapteyn, M. M. Murnane, *Proc. Natl. Acad. Sci. USA* **2010**, *107*, 20219.
- [6] A. Ghosh, R. K. Chaudhuri, S. Chattopadhyay, *J. Chem. Phys.* **2016**, *145*, 124303.
- [7] C. A. Gaggioli, L. Belpassi, F. Tarantelli, J. N. Harvey, P. Belanzoni, *Chem. Eur. J.* **2018**, *24*, 5006–5015.
- [8] X. Krokidis, S. Noury, B. Silvi, *J. Phys. Chem. A* **1997**, *101*, 7277–7282.
- [9] J. Ribas-Arino, D. Marx, *Chem. Rev.* **2012**, *112*, 5412–5487.
- [10] L. Zhao, M. Hermann, W. H. E. Schwarz, G. Frenking, *Nat. Rev. Chem.* **2019**, *3*, 48–63.
- [11] J. Grunenberg, *Chem. Eur. J.* **2016**, *22*, 18678–18681.
- [12] S. Pratihari, X. Ma, Z. Homayoon, G. L. Barnes, W. L. Hase, *J. Am. Chem. Soc.* **2017**, *139*, 3570–3590.
- [13] G. J. Cheng, X. Zhang, L. W. Chung, L. Xu, Y. D. Wu, *J. Am. Chem. Soc.* **2015**, *137*, 1706–1725.
- [14] B. K. Carpenter, *Chem. Rev.* **2013**, *113*, 7265–7286.
- [15] J. Ferrante, J. R. Smith, J. H. Rose, *Phys. Rev. Lett.* **1983**, *50*, 1385–1386.
- [16] J. R. Smith, H. Schlosser, W. Leaf, J. Ferrante, J. H. Rose, *Phys. Rev. A* **1989**, *39*, 514–517.
- [17] J. Ferrante, H. Schlosser, J. R. Smith, *Phys. Rev. A* **1991**, *43*, 3487–3494.
- [18] V. G. Baonza, M. Taravillo, M. Cáceres, J. Núñez, *Phys. Rev. B* **1996**, *53*, 5252–5258.
- [19] A. Toro-Labbé, S. Gutiérrez-Oliva, J. S. Murray, P. Politzer, *Mol. Phys.* **2007**, *105*, 2619–2625.
- [20] P. Politzer, A. Toro-Labbé, S. Gutiérrez-Oliva, B. Herrera, P. Jaque, M. C. Concha, J. S. Murray, *J. Chem. Sci.* **2005**, *117*, 467–472.
- [21] P. Jaque, A. Toro-Labbé, P. Politzer, P. Geerlings, *Chem. Phys. Lett.* **2008**, *456*, 135–140.
- [22] J. Grunenberg, *Int. J. Quantum Chem.* **2017**, *117*, e25359.
- [23] M. Grandbois, M. Beyer, M. Rief, H. Clausen-Schaumann, H. E. Gaub, *Science* **1999**, *283*, 1727–1730.
- [24] M. K. Beyer, *J. Chem. Phys.* **2000**, *112*, 7307–7312.
- [25] P. Huxley, D. B. Knowles, J. N. Murrell, J. D. Watts, *J. Chem. Soc. Faraday Trans.* **1984**, *80*, 1349–1361.
- [26] P. Huxley, J. N. Murrell, *J. Chem. Soc. Faraday Trans.* **1983**, *79*, 323–328.
- [27] R. Rydberg, *Z. Phys.* **1932**, *73*, 376–386.
- [28] O. Klein, *Z. Phys.* **1932**, *76*, 226–246.
- [29] G. L. A. Rees, *Proc. Phys. Soc.* **1947**, *59*, 998–1010.
- [30] P. Politzer, J. S. Murray, P. Lane, A. Toro-Labbé, *Int. J. Quantum Chem.* **2007**, *107*, 2153–2157.
- [31] J. S. Murray, A. Toro-Labbé, T. Clark, P. Politzer, *J. Mol. Model.* **2009**, *15*, 701–706.
- [32] D. Cremer, A. Wu, A. Larsson, E. Kraka, *J. Mol. Model.* **2000**, *6*, 396–412.
- [33] M. Kaupp, B. Metz, H. Stoll, *Angew. Chem. Int. Ed.* **2000**, *39*, 4607–4609; *Angew. Chem.* **2000**, *112*, 4780–4782.
- [34] E. Kraka, D. Setiawan, D. Cremer, *J. Comput. Chem.* **2016**, *37*, 130–142.
- [35] G. S. Hammond, *J. Am. Chem. Soc.* **1955**, *77*, 334–338.
- [36] R. F. W. Bader, *Atoms in molecules. A quantum theory*, Oxford University Press, New York, **1994**.
- [37] R. F. W. Bader, *J. Phys. Chem. A* **2010**, *114*, 7431–7444.
- [38] M. Rahm, K. O. Christe, *ChemPhysChem* **2013**, *14*, 3714–3725.
- [39] A. Savin, R. Nesper, S. Wengert, T. E. Fassler, *Angew. Chem. Int. Ed. Engl.* **1997**, *36*, 1808–1832; *Angew. Chem.* **1997**, *109*, 1892–1918.
- [40] Y. Tal, R. F. W. Bader, T. T. Nguyen-Dang, M. Ojha, S. G. Anderson, *J. Chem. Phys.* **1981**, *74*, 5162–5167.
- [41] S. Berski, J. Andrés, B. Silvi, L. R. Domingo, *J. Phys. Chem. A* **2006**, *110*, 13939–13947.
- [42] J. Contreras-García, A. M. Pendás, J. M. Recio, *J. Phys. Chem. B* **2008**, *112*, 9787–9794.
- [43] M. A. Salvadó, P. Pertierra, A. Morales-García, J. M. Menéndez, J. M. Recio, *J. Phys. Chem. C* **2013**, *117*, 8950–8958.
- [44] M. Miao, Y. Sun, E. Zurek, H. Lin, *Nat. Rev. Chem.* **2020**, *4*, 508–527.
- [45] M. Rahm, R. Cammi, N. W. Ashcroft, R. Hoffmann, *J. Am. Chem. Soc.* **2019**, *141*, 10253–10271.
- [46] M. Miao, R. Hoffmann, *J. Am. Chem. Soc.* **2015**, *137*, 3631–3637.
- [47] Á. Lobato, H. H. Osman, M. A. Salvadó, P. Pertierra, Á. Vegas, V. G. Baonza, J. M. Recio, *Inorg. Chem.* **2020**, *59*, 5281–5291.
- [48] A. M. Pendás, M. A. Blanco, A. Costales, P. M. Sánchez, V. Luaña, *Phys. Rev. Lett.* **1999**, *83*, 1930–1933.
- [49] L. A. Terrabuio, T. Q. Teodoro, C. F. Matta, R. L. A. Haiduke, *J. Phys. Chem. A* **2016**, *120*, 1168–1174.
- [50] T. Stuyver, S. Shaik, *J. Am. Chem. Soc.* **2020**, *142*, 20002–20013.
- [51] A. C. West, M. W. Schmidt, M. S. Gordon, K. Ruedenberg, *J. Phys. Chem. A* **2015**, *119*, 10360–10367.
- [52] E. Sheka in *Advances in Quantum Chemistry*, Vol. 70 (Eds.: J. R. Sabin, E. J. Brändas), Academic Press, New York, **2015**, pp. 111–161.

- [53] M. Fuchs, Y. M. Niquet, X. Gonze, K. Burke, *J. Chem. Phys.* **2005**, *122*, 094116.
- [54] J. P. Perdew, A. Ruzsinszky, J. Sun, N. K. Nepal, A. D. Kaplan, *Proc. Natl. Acad. Sci. USA* **2021**, *118*, e2017850118.
- [55] K. Boguslawski, P. Tecmer, Ö. Legeza, M. Reiher, *J. Phys. Chem. Lett.* **2012**, *3*, 3129–3135.
- [56] J. Andrés, S. Berski, B. Silvi, *Chem. Commun.* **2016**, *52*, 8183–8195.
- [57] R. Thom, *Structural stability and morphogenesis: An outline of a general theory of models*, W. A. Benjamin, New York, **1975**.
- [58] R. Isea, *J. Mol. Struct.* **2001**, *540*, 131–138.
- [59] C. R. Groom, I. J. Bruno, M. P. Lightfoot, S. C. Ward, *Acta Crystallogr. Sect. B* **2016**, *72*, 171–179.
- [60] J. Li, R. Pang, Z. Li, G. Lai, X.-Q. Xiao, T. Müller, *Angew. Chem. Int. Ed.* **2019**, *58*, 1397–1401; *Angew. Chem.* **2019**, *131*, 1411–1415.
- [61] L. R. Domingo, *RSC Adv.* **2014**, *4*, 32415–32428.
- [62] L. R. Domingo, E. Chamorro, P. Pérez, *Org. Biomol. Chem.* **2010**, *8*, 5495–5504.
- [63] D. R. Huntley, G. Markopoulos, P. M. Donovan, L. T. Scott, R. Hoffmann, *Angew. Chem. Int. Ed.* **2005**, *44*, 7549–7553; *Angew. Chem.* **2005**, *117*, 7721–7725.
- [64] F. Occelli, P. Loubeyre, R. LeToullec, *Nat. Mater.* **2003**, *2*, 151–154.
- [65] M. Martínez-Canales, C. J. Pickard, R. J. Needs, *Phys. Rev. Lett.* **2012**, *108*, 045704.
- [66] F. Wang, *J. Mol. Struct.* **2003**, *664–665*, 83–89.
- [67] F. Fantuzzi, T. M. Cardozo, M. A. C. Nascimento, *Phys. Chem. Chem. Phys.* **2017**, *19*, 19352–19359.
- [68] M. Fu, S. Pan, L. Zhao, G. Frenking, *J. Phys. Chem. A* **2020**, *124*, 1087–1092.
- [69] E. Espinosa, I. Alkorta, J. Elguero, E. Molins, *J. Chem. Phys.* **2002**, *117*, 5529–5542.
- [70] E. Espinosa, E. Molins, *J. Chem. Phys.* **2000**, *113*, 5686–5694.
- [71] S. J. Grabowski, *Chem. Rev.* **2011**, *111*, 2597–2625.
- [72] B. Silvi, H. Ratajczak, *Phys. Chem. Chem. Phys.* **2016**, *18*, 27442–27449.
- [73] F. Weinhold, R. A. Klein, *Mol. Phys.* **2012**, *110*, 565–579.
- [74] P. M. Dominiak, A. Makal, P. R. Mallinson, K. Trzcinska, J. Eilmes, E. Grech, M. Chruszcz, W. Minor, K. Wozniak, *Chem. Eur. J.* **2006**, *12*, 1941–1949.
- [75] P. R. Mallinson, G. T. Smith, C. C. Wilson, E. Grech, K. Wozniak, *J. Am. Chem. Soc.* **2003**, *125*, 4259–4269.
- [76] P. Pyykkö, M. Atsumi, *Chem. Eur. J.* **2009**, *15*, 186–197.
- [77] S. Alvarez, *Dalton Trans.* **2013**, *42*, 8617–8636.
- [78] I. Dance, *New J. Chem.* **2003**, *27*, 22–27.
- [79] M. Rahm, R. Hoffmann, N. W. Ashcroft, *Eur. J. Chem.* **2016**, *22*, 14625–14632.
- [80] F. Cordero, V. Gomez, A. E. Platero-Prats, M. Reves, J. Echeverria, E. Cremades, F. Barragan, S. Alvarez, *Dalton Trans.* **2008**, 2832–2838.

Manuscript received: February 28, 2021

Accepted manuscript online: April 12, 2021

Version of record online: June 22, 2021